Ceiling- or Wall-Mounted Access Points: An Experimental Evaluation for Indoor Millimeter Wave Communications

Yoo, S. K., Zhang, L., Cotton, S., Ngo, H. & Scanlon, W.

ISBN 9788890701887

Publisher: IEEE

Ceiling- or Wall-Mounted Access Points: An Experimental Evaluation for Indoor Millimeter Wave Communications

Seong Ki Yoo, Lei Zhang, Simon L. Cotton, Hien Quoc Ngo and William G. Scanlon
Centre for Wireless Innovation, ECIT Institute, Queen's University Belfast, BT3 9DT, UK
{sk.yoo, lzhang27, simon.cotton, hien.ngo, w.scanlon}@qub.ac.uk

***Abstract*—This paper compares the received signal characteristics obtained for two access point (AP) mounting arrangements commonly encountered in indoor millimeter wave wireless networks, namely ceiling- and wall-mounted APs. To facilitate this, we consider three key user equipment (UE) usage scenarios, in which a user imitated making a voice call, operating an app and carrying the device in a pocket. For each of these UE cases, we investigate the fading characteristics of the millimeter wave channel at 60 GHz as the user walk toward and then away from the ceiling- and wall-mounted APs. Following this, the lognormal and κ-μ distributions are shown to provide a good fit to the shadowed and multipath fading, respectively. Based on the parameter estimates and model fitting, it is found that the choice between a ceiling- and wall-mounted position for the AP is dependent on the UE use case and whether the device is in line-of-sight (LOS) or non-LOS (NLOS).**

***Index Terms*— κ-μ model, lognormal model, millimeter wave, multipath fading, shadowed fading.**

I. Introduction

Within the millimeter wave (mmWave) region of the radio spectrum, the unlicensed 60 GHz band provides up to 7 GHz of unlicensed spectrum worldwide, providing the potential to develop wireless communication systems with multi-Gbps throughput [1]. With this in mind, the 60 GHz band has been proposed as a promising candidate for the next generation multi-gigabit wireless local area networks (WLANs) [2]. However, it is also well known that signal transmissions at mmWave frequencies are particularly vulnerable to the shadowing (or equivalently signal blockage) caused by different obstacles (e.g., people, objects, user) and user mobility. In particular, these effects can be more prominent when mmWave devices are operated in close proximity to the user's body [3].

A number of studies have been performed to understand these deleterious effects [4–9]. For example, in [4], the authors analyzed the blockage capacity of the radio link between the user equipment (UE) and ceiling-mounted access point (AP) in an indoor environment. It was shown that the probability of a line-of-sight (LOS) link between the UE and AP being blocked increased as the UE moved towards the edge of the service area. To overcome the blockage, a number of different techniques, namely spatial diversity [5], multi-hop relay [6] and multiple APs [7], have been pursued. All of these approaches have been shown to provide an improvement in the link quality when the direct LOS signal path was blocked. The authors of [8] investigated the handover between the APs for mmWave communications and found out that the performance can be improved if the mobility direction and velocity of the user are known. In [9], a high gain steerable antennas were employed to overcome large propagation losses and realize a reliable communication link. All of these studies have provided important insights into how many of the adverse propagation phenomena may be overcome for indoor mmWave communications. Nevertheless, none of these studies have performed an explicit comparison of the fading characteristics observed by APs when mounted on either a ceiling or wall.

To address this issue, the authors of [10] compared three different AP locations (ceiling, corner and wall) for indoor wireless communications operating at 37.2 GHz using propagation loss and ray-tracing models when the direct signal path between the transmitter (TX) and receiver (RX) was obstructed by a human, i.e., non-LOS (NLOS) link. It was found that the wall-mounted AP provided the best channel performance. However, this study was limited to a consideration of fixed TX and RX locations only and thus it is difficult to see how the results can be extrapolated for the cases when either the TX or RX is operated near the human body while the user is mobile. Therefore, in this study, we empirically investigate and compare the fading characteristics of the received signal at two popular AP locations, namely ceiling and wall positions. In particular, we decompose the received signal into its shadowed and multipath fading and compare the severity of both types of fluctuation for the ceiling- and wall-mounted APs.

It is worth highlighting that the indoor mmWave channel measurements at 60 GHz presented in this paper and [3] were performed in the same hallway environment. However, in [3], the effect of user handling upon the UE to eNB (or equivalently AP) channel was mainly investigated to provide a better understanding of the impact of different UE operations on the channel. In contrast, as stated above, the main objective of this study is to investigate and compare the fading characteristics of the received signal at two different AP mounting positions. Consequently, the hypothesis, measurements and analysis used in this paper and [3] have an entirely different focus.

II. Measurement Set-up and Experiments

A. Measurement Set-up

The hypothetical UE used for the mmWave channel measurements consisted of a Hittite HMC6000LP711E TX mod-

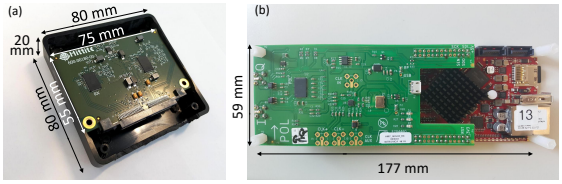

Fig. 1. Hypothetical (a) UE and (b) AP used for the measurements along with their dimensions.

ule containing on-chip, low profile antenna with a gain of +7.5 dBi [11]. A continuous wave (CW) tone of 50 MHz baseband frequency was fed into a 90° splitter to provide the analogue baseband I/Q signal. This configuration enabled us to transmit a narrowband signal centered at 60.05 GHz using at an Equivalent Isotropically Radiated Power (EIRP) of +10.9 dBm. The TX module was fixed to the inside of a compact acrylonitrile butadiene styrene enclosure (80 mm × 80 mm × 20 mm) to emulate a hypothetical UE (Fig. 1(a)).

As shown in Fig. 1(b), the hypothetical AP used for the mmWave channel measurements was based on a Hittite HMC 6001LP711E mmWave RX module [12] which featured on-chip low profile antennas with +7.5 dBi gain with the normalized free-space radiation patterns presented in [13]. The 50 MHz intermediate frequency (IF) signal outputted by the RX module was sampled using a v1.4 Red Pitaya data acquisition platform. The Red Pitaya v1.4 contains a 14-bit, 125 Msps analog-to-digital converter (ADC) which was connected to a field programmable gate array (FPGA). The FPGA unit was programmed with a custom direct digital down conversion implementation based on the embedded SDR receiver described in [14]. This implementation provided an effective channel sampling frequency of 2 kHz and a receive bandwidth of 86 kHz. As shown in Fig. 2, the wall-mounted AP was located on the wall at a height of 2.50 m above floor level using a small strip of Velcro® whereas the ceiling-mounted AP was placed above the ceiling tile at a height of 2.70 m above floor level with the antenna boresight oriented towards the floor. It is remarking that the mmWave channel measurements between the UE and two APs were performed simultaneously for a direct cross-comparison of the fading characteristics observed at both AP locations.

B. Experiments

The measurements were conducted within an indoor hallway environment which is located on the 1st floor of the ECIT Institute at Queen's University Belfast in the United Kingdom (Fig. 2). The indoor environment featured metal studded dry walls with a metal tiled floor covered with polypropylene-fiber, rubber backed carpet tiles, and metal ceiling with mineral fiber tiles and recessed louvered luminaries suspended 2.70 m above floor level. It is worth remarking that the hallway environment was unoccupied for the duration of the measurements. During the measurements, an adult male of height of 1.83 m and mass 78 kg imitated three different use cases which are likely to be representative of everyday UE usage. These were: (1) making a voice call, where the user held the UE at his right ear; (2) operating an app, where the user held the UE with his two hands in front of his body; (3) carrying a device, where the UE was located in the right-front pocket of the user's clothing. Herein, and for brevity, we denote the three different UE usage cases as *head*, *hand* and *pocket*, respectively.

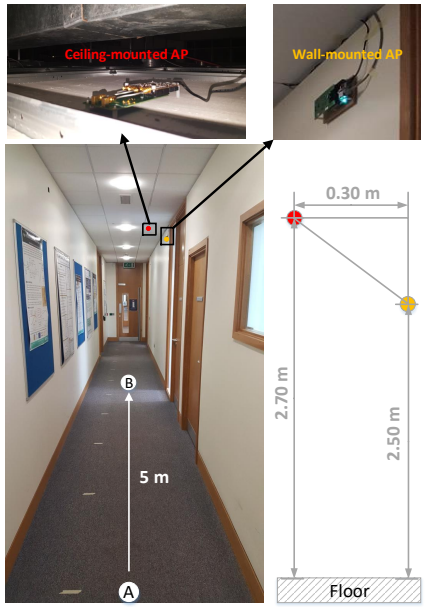

Fig. 2. Indoor hallway environment along with the location of ceiling- and wall-mounted APs.

In this study, we considered two different channel conditions, namely, (1) mobile LOS and (2) mobile non-LOS (NLOS) channel conditions, where the user walked towards (path AB) and away from (path BA) the hypothetical AP in a straight line, respectively. The considered walking distance for both the LOS and NLOS scenarios was 5 m. To improve the validity and robustness of the parameter estimates obtained in this study, all the measurements were repeated five times. The average walking speed maintained by the user throughout all of the experiments was approximately 1.0 m/s.

III. Shadowed and Multipath Fading Models

In wireless communications channels, the path loss, shadowed and multipath fading are mainly responsible for shaping the characteristics of the received signal. The path loss is a measure of the signal attenuation between the TX and RX and is a function of the separation distance. Multipath fading is caused by the constructive and destructive interference of radio waves while the shadowed fading is precipitated by the presence of obstructions between the TX and RX. There have been a number of different models used to describe the statistical behavior of the shadowed and multipath fading experienced in mobile radio propagation channels [15–18]. In this study, we considered the lognormal and κ-μ distributions for shadowed and multipath fading, respectively.

A. Lognormal Distribution

The shadowed fading is often modeled using the lognormal distribution which has been shown to provide a good fit to the

data obtained in empirical studies [15], [16]. The probability density function (PDF) of the shadowed fading envelope, R_s, in a lognormal channel can be expressed as follows

$$f_{R_s}(r_s;u,\sigma)=\frac{1}{r_s\sqrt{2\pi\sigma^2}}\exp\left[-\frac{\left(\ln r_s-u\right)^2}{2\sigma^2}\right] \quad (1)$$

where u and σ represent the mean and standard deviation, respectively.

B. κ-μ Distribution

The κ-μ distribution has been proposed as a generalized statistical model which may be used to represent the random variation of the multipath fading signal [19] and includes Rayleigh, Rice and Nakagami-m as special cases. Moreover, the authors of [13] recommended the use of the κ-μ distribution to fully take into account signal reception through multipath as well as any LOS component for the UE to AP channels. The PDF of the multipath fading signal envelope, R_m, in a κ-μ fading channel can be expressed as

$$f_{R_m}(r_m)=\frac{2\mu(\kappa+1)^{\frac{\mu+1}{2}}{r_m}^{\mu}}{\kappa^{\frac{\mu-1}{2}}\exp\left(\mu\kappa\right)\Omega^{\frac{\mu+1}{2}}}\exp\left(\frac{-\mu\left(\kappa+1\right){r_m}^2}{\Omega}\right) \times I_{\mu-1}\left(2\mu\sqrt{\kappa\left(\kappa+1\right)}\frac{r_m}{\sqrt{\Omega}}\right) \quad (2)$$

where $I_v(\cdot)$ represents the modified Bessel function of the first kind with order v. In terms of its physical interpretation, κ is defined as the ratio between the total power in the dominant signal components and the total power in the scattered signal components, μ is related to the number of multipath clusters and Ω is the mean signal power given by $\Omega=\mathbb{E}[R_m^2]$ with $\mathbb{E}[\cdot]$ denoting the expectation operator. It is recalled here that the amount of fading (AF) is often used as a relative measure of the severity of fading encountered in wireless transmission over fading channels [20]. This can be obtained as $AF=(1+2\kappa)/\mu(1+\kappa)^2$ for the case of a κ-μ fading channel [19].

IV. Results

The shadowed fading was extracted from the received signal power by first removing the estimated path loss using the approach described in [21]. Then, the resultant data set was averaged using a moving window of 100 channel samples (equivalent to a distance of 10 wavelengths). The parameter estimates for the lognormal model were obtained using maximum likelihood estimation (MLE) performed in MATLAB along with the PDF given in (1). On the contrary, multipath fading was extracted by removing both the path loss and shadowed fading from the measurement data as detailed above. Then, the parameter estimates for the κ-μ fading model were performed using the non-linear least squares programmed in MATLAB along with the PDF given in (2). It is worth highlighting that the received signal power was converted to amplitude prior to the parameter estimation process.

A. Head Position

Table I shows the mean values of the parameter estimates of the lognormal and κ-μ models averaged over the five repeated trials along with the estimated AFs. Using the same method adopted in [22], the standard deviation of the lognormal distribution is presented in dB, which represents the depth of shadowed fading. As we can see, σ_{dB} for the ceiling-mounted AP was smaller than that for the wall-mounted AP for both the LOS and NLOS walking cases. For both the ceiling- and wall-mounted APs, the κ parameter estimates were greater than unity ($\kappa>1$) for the LOS links, suggesting that there existed strong dominant signal components. In contrast, for the NLOS links, the κ parameter estimates were slightly less than unity ($\kappa<1$). Accordingly, for both the ceiling- and wall-mounted APs, the estimated AF for the LOS links was less than that for the NLOS links. When comparing the AF for the ceiling- and wall-mounted APs, for the LOS links, the severity of fading observed in the ceiling-mounted AP is less (i.e., smaller value of AF) compared to that of the wall-mounted AP. On the contrary, for the NLOS links, the wall-mounted AP experience less fading compared to the ceiling-mounted AP. As an example of the model fitting process, Fig. 3 shows the respective PDFs of the lognormal and κ-μ distributions fitted to the shadowed and multipath fading observed in the NLOS walking scenarios during the 1st trial. It is apparent that both models provided an excellent fit to the measured data.

B. Hand Position

As shown in Table I, σ_{dB} for the ceiling-mounted AP was greater than that for the wall-mounted AP for the LOS case whereas σ_{dB} for the ceiling-mounted AP was smaller than that for the wall-mounted AP for the NLOS case. For both the ceiling- and wall-mounted APs, the κ parameter estimates were greater than unity for the LOS links. Interestingly, the κ parameter estimates were found to be greater than unity ($\kappa>1$) even for the NLOS links, suggesting that there existed strong signal components even for the NLOS walking scenarios. This was presumably due to the fact that the UE was held a short distance in front of the body and may have benefited from reduced body induced shadowing. Fig. 4 presents the empirical PDFs of the shadowed and multipath fading observed in the LOS walking scenarios during the 3rd trial alongside the respective lognormal and κ-μ PDFs. It can easily be seen that the lognormal and κ-μ distributions provided a good fit to the measured shadowed and multipath fading, respectively. When comparing PDFs for the ceiling- and wall-mounted APs, they were found to be very similar each other in terms of the shadowed fading (Fig. 4(a)) while the ceiling-mounted AP is subject to less multipath fading compared to the wall-mounted AP (Fig. 4(b)).

C. Pocket Position

For the pocket position, the ceiling-mounted AP had greater values of σ_{dB} compared to the wall-mounted AP for both the LOS and NLOS walking cases. For both the ceiling- and wall-mounted APs, the κ parameter estimates were greater than unity ($\kappa>1$) for the LOS links. Nevertheless, the ceiling-mounted AP had much stronger dominant signal components compared to the wall-mounted AP for the LOS links and

TABLE I
AVERAGE PARAMETER ESTIMATES FOR THE LOGNORMAL AND κ-μ MODELS FOR THE LOS AND NLOS WALKING SCENARIOS WITH THE HEAD, HAND AND POCKET POSITIONS ALONG WITH THE ESTIMATED AFS.

UE Cases	AP Locations	LOS						NLOS					
		u	σ_{dB}	κ	μ	Ω	AF	u	σ_{dB}	κ	μ	Ω	AF
Head	Wall	-0.13	2.8	1.81	0.89	1.19	0.66	-0.05	1.8	0.97	0.99	1.22	0.77
	Ceiling	-0.06	2.5	2.22	0.86	1.17	0.61	-0.01	1.6	0.92	0.96	1.23	0.80
Hand	Wall	-0.09	2.0	1.21	0.95	1.21	0.74	-0.18	3.4	2.69	0.76	1.17	0.62
	Ceiling	-0.07	2.4	2.37	0.83	1.17	0.62	-0.10	2.2	1.62	0.88	1.20	0.70
Pocket	Wall	-0.07	2.8	3.94	0.67	1.14	0.55	-0.07	1.8	0.48	1.01	1.25	0.88
	Ceiling	-0.04	3.1	368.34	0.11	1.09	0.38	-0.06	2.1	0.47	1.01	1.25	0.89

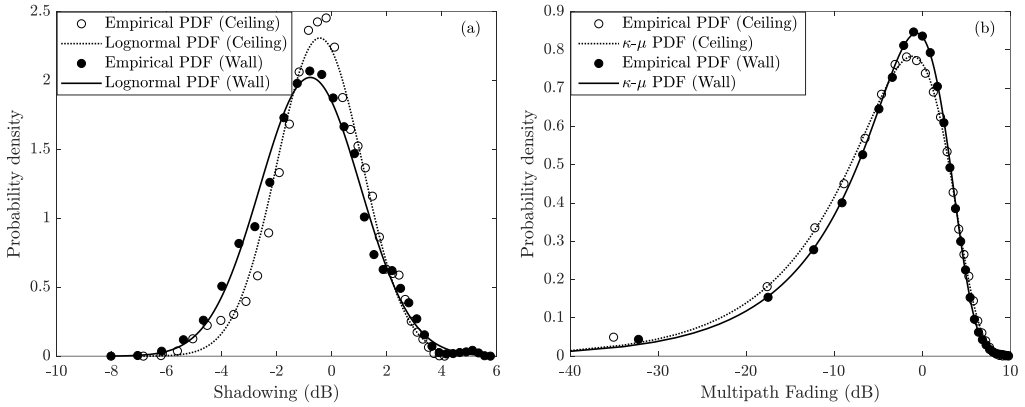

Fig. 3. Empirical (symbols), theoretical lognormal (dotted lines) and κ-μ (continues lines) PDFs of the (a) shadowed and (b) multipath fading observed in the NLOS walking scenarios during the 1st trial for the head position.

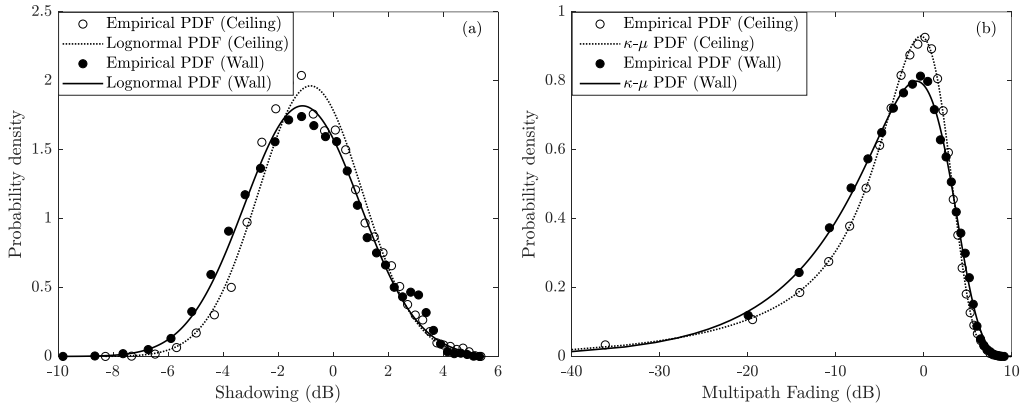

Fig. 4. Empirical (symbols), theoretical lognormal (dotted lines) and κ-μ (continues lines) PDFs of the (a) shadowed and (b) multipath fading observed in the LOS walking scenarios during the 3rd trial for the hand position.

subsequently a smaller value of AF for the ceiling-mounted AP. More specifically, very strong dominant signal components ($\kappa >> 1$) and little scattered multipath ($\mu \to 0$) was observed in the LOS UE to ceiling-mounted AP link. This suggests that the fluctuations of the signal envelope observed in the LOS pocket UE to ceiling-mounted AP link were similar to those expected for extreme κ-μ fading channels [23].

For the NLOS channel conditions, the mean values of the κ parameters were found to be 0.47 and 0.48 for the ceiling- and wall-mounted APs, respectively, indicating no strong dominant signal components. This was most likely due to the fact that the direct signal path between the pocket UE and APs was obstructed by the user's body. Additionally, the μ parameter estimates were found to be very close to unity ($\mu = 1$). It is recalled that the κ-μ fading model coincides with the Rayleigh fading model when $\kappa = 0$ and $\mu = 1$. Consequently, it can be inferred that for both the ceiling- and wall-mounted APs the multipath fading conditions observed in the NLOS links are slightly better than those found in a Rayleigh fading environment. When comparing the parameter estimates and AFs for the ceiling- and wall-mounted APs for the NLOS links, they were very similar each other. Furthermore, similar to the head position, the mean values of the AF for the LOS links were less than those for the NLOS links for both the ceiling- and wall-mounted APs.

As an example of the model fits, Fig. 5 shows the good fits of the lognormal and κ-μ models to the shadowed and multipath fading experienced in the LOS walking scenarios

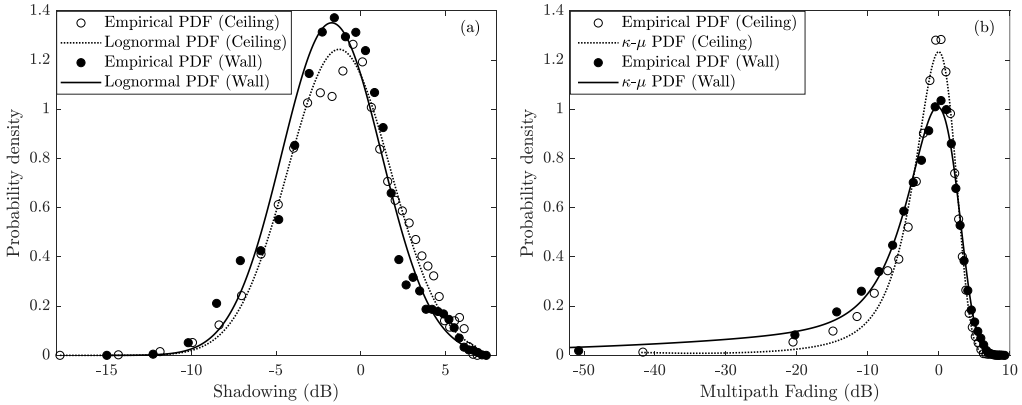

Fig. 5. Empirical (symbols), theoretical lognormal (dotted lines) and κ-μ (continues lines) PDFs of the (a) shadowed and (b) multipath fading observed in the LOS walking scenarios during the 2nd trial for the pocket position.

during the 2nd trial. Again, in agreement with the parameter estimates, the wall-mounted AP is subject to slightly less shadowed fading compared to the ceiling-mounted AP whereas the ceiling-mounted AP is subject to less multipath fading compared to the wall-mounted AP.

V. Conclusion

In this paper, the fading characteristics observed in the links between the hypothetical UE and ceiling- and wall-mounted APs operating in indoor mmWave communications channels at 60 GHz were empirically investigated and compared. To this end, the channel measurements were carried out in an indoor hallway environment under mobile LOS and NLOS conditions with three different UE positions. Over all of the measurements, the lognormal and κ-μ models provided a good fit to the shadowed and multipath fading observed in UE to APs channels. Based on the parameter estimates, it may be concluded that the choice between two AP locations will come down to the UE positions (i.e., UE usage cases) and the user movement (i.e., how the UE is operated or carried by the user).

Acknowledgment

This work was supported by the Engineering and Physical Sciences Research Council under Grant Reference EP/L026074/1 and the Department for Employment and Learning Northern Ireland through Grant Reference USI080.

References

[1] R. C. Daniels and R. W. Heath Jr, "60 GHz wireless communications: Emerging requirements and design recommendations," *IEEE Veh. Technol. Mag.*, vol. 2, no. 3, pp. 41–50, Sep. 2007.

[2] C. Park and T. S. Rappaport, "Short-range wireless communications for next-generation networks: UWB, 60 GHz millimeter-wave WPAN, and ZigBee," *IEEE Wireless Commun.*, vol. 14, no. 4, pp. 70–78, Aug. 2007.

[3] S. K. Yoo, S. L. Cotton, R. W. Heath Jr, and Y. J. Chun, "Measurements of the 60 GHz UE to eNB channel for small cell deployments," *IEEE Wireless Commun. Lett.*, vol. 6, no. 2, pp. 178–181, Apr. 2017.

[4] K. Dong, X. Liao, and S. Zhu, "Link blockage analysis for indoor 60GHz radio systems," *IET Electron. Lett.*, vol. 48, no. 23, pp. 1506–1508, 2012.

[5] M. Park and H. K. Pan, "A spatial diversity technique for IEEE 802.11 ad WLAN in 60 GHz band." *IEEE Commun. Lett.*, vol. 16, no. 8, pp. 1260–1262, Aug. 2012.

[6] S. Singh, F. Ziliotto, U. Madhow, E. M. Belding, and M. Rodwell, "Blockage and directivity in 60 GHz wireless personal area networks: From cross-layer model to multihop MAC design," *IEEE J. Select. Areas Commun.*, vol. 27, no. 8, Oct. 2009.

[7] X. Zhang, S. Zhou, X. Wang, Z. Niu, X. Lin, D. Zhu, and M. Lei, "Improving network throughput in 60GHz WLANs via multi-AP diversity," in *Proc. IEEE ICC*, Jun. 2012, pp. 4803–4807.

[8] B. Van Quang, R. V. Prasad, I. Niemieeger, and N. T. V. Huong, "A study on handoff issues in radio over fiber network at 60 GHz," in *Proc. ICCE*, Aug. 2010, pp. 50–54.

[9] A. Maltsev, R. Maslennikov, A. Sevastyanov, A. Khoryaev, and A. Lomayev, "Experimental investigations of 60 GHz WLAN systems in office environment," *IEEE J. Sel. Areas Commun.*, vol. 27, no. 8, pp. 1488–1499, Oct. 2009.

[10] M. Ghaddar, L. Talbi, and T. Denidni, "Investigation of BS antenna location for future indoor wireless mm-wave communication systems," in *Proc. IEEE APSURSI*, Jun. 2003, pp. 110–113.

[11] Analog Device, visited on 10/24/2018. [Online]. Available: http://www.analog.com/media/en/technical-documentation/data-sheets/hmc6000.pdf.

[12] Analog Device, visited on 10/24/2018. [Online]. Available: http://www.analog.com/media/en/technical-documentation/data-sheets/hmc6001.pdf.

[13] S. K. Yoo, S. L. Cotton, Y. J. Chun, and W. G. Scanlon, "Fading characterization of UE to ceiling-mounted access point communications at 60 GHz," *presented at EuCAP 2018*.

[14] Red Pitaya Notes, visited on 10/12/2018. [Online]. Available: http://pavel-demin.github.io/red-pitaya-notes/.

[15] J. Zhu, H. Wang, and W. Hong, "Large-scale fading characteristics of indoor channel at 45-GHz band," *IEEE Antennas Wireless Propag. Lett.*, vol. 14, pp. 735–738, Dec. 2015.

[16] E. Tanghe, W. Joseph, L. Verloock, L. Martens, H. Capoen, K. Van Herwegen, and W. Vantomme, "The industrial indoor channel: Large-scale and temporal fading at 900, 2400, and 5200 MHz," *IEEE Trans. Wireless Commun.*, vol. 7, no. 7, pp. 2740–2751, Jul. 2008.

[17] W. R. Braun and U. Dersch, "A physical mobile radio channel model," *IEEE Trans. Veh. Technol.*, vol. 40, no. 2, pp. 472–482, May 1991.

[18] R. J. Bultitude, S. A. Mahmoud, and W. A. Sullivan, "A comparison of indoor radio propagation characteristics at 910 MHz and 1.75 GHz," *IEEE J. Sel. Areas Commun.*, vol. 7, no. 1, pp. 20–30, Jan. 1989.

[19] M. D. Yacoub, "The κ-μ distribution and the η-μ distribution," *IEEE Antennas Propag. Mag.*, vol. 49, no. 1, pp. 68–81, Feb. 2007.

[20] M. K. Simon and M.-S. Alouini, *Digital communication over fading channels*. New York, NY, USA: Wiley, 2005.

[21] N. Jaldén, P. Zetterberg, B. Ottersten, A. Hong, and R. Thoma, "Correlation properties of large scale fading based on indoor measurements," in *Proc. WCNC*, Mar. 2007, pp. 1894–1899.

[22] A. Abdi and M. Kaveh, "On the utility of gamma PDF in modeling shadow fading (slow fading)," in *Proc. IEEE VTC*, vol. 3, May 1999, pp. 2308–2312.

[23] G. S. Rabelo, U. S. Dias, and M. D. Yacoub, "The κ-μ extreme distribution: Characterizing severe fading conditions," in *Proc. IEEE IMOC*, Nov. 2009, pp. 244–248.